A Switched-Capacitorless Energy-Encrypted Transmitter for Roadway-Charging Electric Vehicles

Wei Liu[1], *Student Member, IEEE*, K.T. Chau[1], *Fellow IEEE*, Christopher H.T. Lee[1, 2], *Member IEEE*, Chaoqiang Jiang[1], *Student Member, IEEE*, and Wei Han[1], *Student Member, IEEE*

[1]Department of Electrical and Electronic Engineering, University of Hong Kong, Hong Kong, China
[2]Research Laboratory of Electronics, Massachusetts Institute of Technology, Cambridge, MA 02139 USA

This paper proposes and implements a switched-capacitorless energy-encrypted transmitter and a two-dimensional frequency-and-duration encryption (FDE) technology for roadway-charging electric vehicles (EVs) based on wireless power transfer (WPT). To prevent the encrypted energy package from being illegally decrypted by unauthorized receivers, the proposed two-dimensional chaotic FDE scheme generates a well-defended security key to improve the security performance for the multi-receiver WPT system. Moreover, by introducing a continuously energy-encrypted transmitter without using a switched-capacitor array as well as a hybrid modulation of pulse density modulation and pulse frequency modulation, the proposed FDE-WPT system can offer high energy security while maintaining high efficiency at flexible operating frequencies. Theoretical analysis, computer simulation and experimental results are provided to verify the feasibility of the proposed FDE-WPT system.

***Index Terms*—Switched-capacitorless, frequency-and-duration encryption, roadway-charging, electric vehicles, wireless power transfer.**

I. Introduction

DUE to cleanliness, convenience and high efficiency, wireless power transfer (WPT) technology has been extensively investigated in various fields, such as electric vehicle (EV) wireless charging [1]-[4], wireless motors [5], [6], wireless heating [7] and wireless lighting [8]. Recently, it has further been extended to realize wireless vehicle-to-grid, vehicle-to-home and vehicle-to-vehicle operations [9].

Energy security has been identified as one of the key factors in further development of WPT technology. It is particularly important for roadway-charging EVs [10], [11], because the transmitted energy should only be picked by the authorized receivers whereas it should not be stolen by the unauthorized ones. Recently, although the selective wireless power transfer has delivered wireless power to only one authorized receiver among multi-receivers [12], the illegal receivers may track and lock the fixed operating frequency to steal the wireless power. Besides, an energy encryption strategy has been proposed to realize energy security in the magnetic resonant coupling (MRC) WPT system [13]. However, this encryption scheme desires a switched-capacitor array to discretely adjust the matched capacitance and hence the operating frequency at the transmitter, which suffers from the drawbacks of high voltage stress and low regulation flexibility [14]. To realize the variable operating frequency, a transistor-controlled variable capacitor has been proposed [15]. However, its relatively low efficiency and low power level remain to be solved. Although virtual capacitors [16] and electric springs [17] may offer a potential solution, their high voltage stress across switches and high-speed processing pose new challenges when they are applied to the MRC-WPT system operating at high resonant frequencies. Meanwhile, a series-to-series (SS) topology with fixed values of resonant inductance and capacitance has been identified to exhibit a selective characteristic for multiple loads when operating at the selected receiver's resonant frequency [18]. This mechanism can be newly extended to derive an energy-encrypted transmitter without using a switched-capacitor array for multiple energy receivers such as roadway-charging EVs.

The MRC-WPT system using the SS topology can further utilize ferrite cores to improve the magnetic induction, hence achieving the merit of high coil-to-coil transmission efficiency [19]. Generally, when operating at different encrypted frequencies, hysteresis control is a preferred method to achieve pulse density modulation (PDM), which takes the advantages of fast dynamic response, high reliability and strong stability [20]. Moreover, the concept of hybrid modulation [21] can offer a favorable reference for the hysteresis control in the energy-encrypted WPT system.

The rest of this paper is organized as follows. Section II will discuss the topology and operation principle of the proposed energy-encrypted WPT system. Section III will present the two-dimensional frequency-and-duration (FDE) algorithm and the hybrid modulation. In Section IV, both simulation and experimental results will be given to verify the proposed system. A conclusion will be drawn in Section V.

II. Energy-Encrypted WPT System

Energy encryption technology, as a promising energy security assurance, exhibits a great significance on improving the security performance in various WPT-based applications, especially for park-charging and roadway-charging EVs [14]. Fig. 1 shows the proposed FDE-WPT system without using a switched-capacitor array in the transmitter. The whole system mainly comprises of one transmitter and multiple receivers, including the authorized and unauthorized ones. It is worth noting that the switched-capacitorless transmitter is firstly introduced to the energy-encrypted WPT system, which can offer the definite merit of continuously and flexibly regulating the operating frequency and its active duration.

As depicted in Fig. 1, R_p, L_p, C_p, i_p, R_{sk}, L_{sk}, C_{sk} and i_{sk} (k, m and $n \in Z^+$) with subscripts p and s denote the coil internal

resistances, resonant coil inductances, matched capacitances and currents in the primary and the secondary circuits in the k-th energy-charging channel, respectively. Besides, L_{psk} and $L_{sk_1k_2}$ ($k_1, k_2 \in [1, n]$) denote the mutual inductance between the primary and the k-th secondary coils and that between the k_1-th and k_2-th secondary coils, respectively. Meanwhile, λ_k obeys a random distribution, which represents the number of EVs in the k-th energy-charging channel.

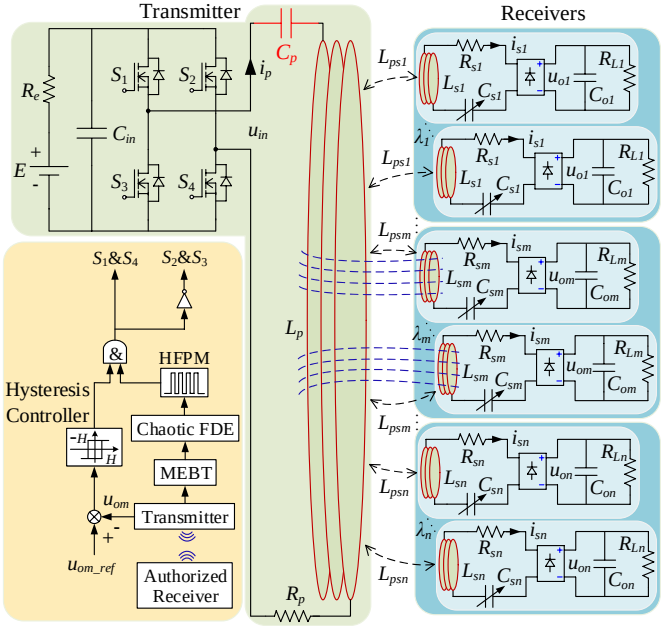

Fig. 1. Proposed FDE-WPT system with switched-capacitorless transmitter.

To commence with theoretical analysis, some assumptions are made: (i) L_{sk}=L_s, L_{psk}=L_{ps}, R_{sk}=R_s, and R_{Lk}=R_L. (ii) R'_{Lk} ($k \neq m$) and R'_{Lm} are the equivalent resistances of load resistances R_{Lk} and R_{Lm}, respectively, and R'_{Lk}=R'_{Lm}=R'_L. (iii) $L_{psk} >> L_{sk_1k_2}$, and $L_{sk_1k_2}$ can be regarded as zero.

When the m-th group of receivers are authorized, both the transmitter and the m-th group of authorized receivers operate at the resonant frequency f_m. Thus, the general equation can be derived as:

$$\begin{bmatrix} Z_p & Z_{ps1}\lambda_1 & Z_{ps2}\lambda_2 & \cdots & Z_{psm}\lambda_m & \cdots & Z_{psn}\lambda_n \\ Z_{ps1} & Z_{s1} & Z_{s12}\lambda_2 & \cdots & Z_{s1m}\lambda_m & \cdots & Z_{s1n}\lambda_n \\ Z_{ps2} & Z_{s12}\lambda_1 & Z_{s2} & \cdots & Z_{s2m}\lambda_m & \cdots & Z_{s2n}\lambda_n \\ \vdots & \vdots & \vdots & \ddots & \vdots & \ddots & \vdots \\ Z_{psm} & Z_{s1m}\lambda_1 & Z_{s2m}\lambda_2 & \cdots & Z_{sm} & \cdots & Z_{smn}\lambda_n \\ \vdots & \vdots & \vdots & \ddots & \vdots & \ddots & \vdots \\ Z_{psn} & Z_{s1n}\lambda_1 & Z_{s2n}\lambda_2 & \cdots & Z_{smn}\lambda_m & \cdots & Z_{sn} \end{bmatrix} \begin{bmatrix} i_p \\ i_{s1} \\ i_{s2} \\ \vdots \\ i_{sm} \\ \vdots \\ i_{sn} \end{bmatrix} = \begin{bmatrix} U_{in} \\ 0 \\ 0 \\ \vdots \\ 0 \\ \vdots \\ 0 \end{bmatrix} \tag{1}$$

where $Z_{psk} = j\omega_m L_{psk}$, $Z_{sk_1k_2} = j\omega_m L_{sk_1k_2}$ and U_{in} is the root-mean-square (RMS) value of the power source u_{in}, and ω_m is the angular frequency corresponding to f_m. Besides, Z_p, Z_{sk} and Z_{sm} denote the impedances of the primary, the k-th and the m-th secondary circuits operating at f_m, respectively. They can be expressed as:

$$\begin{cases} Z_p = R_p + j\omega_m L_p + 1/(j\omega_m C_p) \\ Z_{sk} = R'_{Lk} + R_{sk} + j\omega_m L_{sk} + 1/(j\omega_m C_{sk}),\ k \neq m \\ Z_{sm} = R'_{Lm} + R_{sm} \end{cases} \tag{2}$$

In the primary circuit, the total reflected impedance Z_{ref} from all the secondary circuits and the k-th one Z_{refk} reflected from the k-th secondary circuits can be respectively calculated as:

$$Z_{ref} = \sum_{k=1,\, k\neq m}^{n} \lambda_k Z_{refk} + \lambda_m \frac{(\omega_m L_{psm})^2}{R_{sm} + R'_{Lm}},\ Z_{refk} = \frac{(\omega_m L_{psk})^2}{Z_{sk}} \tag{3}$$

Hence, the total reflected impedance from the unauthorized receivers can be simplified and even neglected by satisfying the following inequality:

$$\lambda_m \frac{(\omega_m L_{psm})^2}{R_{sm} + R'_{Lm}} >> \left| \mathrm{Im}\left(\sum_{k=1,\, k\neq m}^{n} \lambda_k Z_{refk} \right) \right| >> \mathrm{Re}\left(\sum_{k=1,\, k\neq m}^{n} \lambda_k Z_{refk} \right) \tag{4}$$

where Re(·) and Im(·) are the real and imaginary parts of complex impedance, respectively.

Besides, the input impedance angle φ, input power P_{in} and total output power P_{outk} in the k-th energy-charging channel can be respectively derived as:

$$\begin{cases} \varphi = \arctan\left(\mathrm{Im}(Z_p + Z_{ref}) / \mathrm{Re}(Z_p + Z_{ref}) \right) \\ P_{in} = \left| U_{in}^2 / (Z_p + Z_{ref}) \right| \cos\varphi \\ P_{outk} = \lambda_k \left| \omega_m L_{psk} U_{in} / \left(Z_{sk} (Z_p + Z_{ref}) \right) \right|^2 R'_{Lk} \end{cases} \tag{5}$$

Hence, the transmission efficiency η_k in the k-th channel can be derived as:

$$\eta_k = \frac{P_{outk}}{P_{in}} = \frac{\lambda_k R'_{Lk} (\omega_m L_{psk})^2}{|Z_{sk}|^2 \left(\mathrm{Re}\left(\sum_{k=1}^{n} \lambda_k Z_{refk} \right) + R_p \right)} \tag{6}$$

Particularly, when the m-th receivers are authorized, no matter the transmitter operates at resonance or not, the corresponding transmission efficiency can be obtained as:

$$\eta_m = \frac{R'_L}{R + \sum_{k=1,\, k\neq m}^{n} \frac{\lambda_k R^3}{\lambda_m \left[R^2 + (\omega_m L_s - 1/\omega_m C_{sk})^2 \right]} + \frac{R_p R^2}{\lambda_m (\omega_m L_{ps})^2}} \tag{7}$$

where $R = R_s + R'_L$.

Therefore, the transmission efficiencies η_k and η_m are impervious to the primary resonance parameters L_p and C_p. Although the primary coil internal resistance R_p leads to extra power loss, the proposed system takes the advantage of lower transmitter's power loss over the energy-encrypted SS WPT system with switched-capacitor arrays [14].

III. Two-Dimensional Energy Encryption Scheme

As depicted in Fig. 1, the data interaction based on wireless communication facilitates the encryption and decision-making unit to achieve the maximum efficiency band tracking (MEBT). Owing to the dynamic and random changes in the operating frequency of the unauthorized receivers, the MEBT will dynamically produce a new optional frequency band to maximize the transmission efficiency. Then, a two-dimensional

chaotic FDE algorithm is adopted to dynamically generate the encrypted frequency and its active duration sequences – the security keys. Furthermore, the hysteresis control and high-frequency pulse modulation (HFPM), incorporated with two-dimensional FDE, are employed to realize a hybrid modulation of PDM and pulse frequency modulation (PFM).

In Fig. 2, the proposed two-dimensional FDE algorithm comprises of two chaotic sources of the encrypted frequency and active duration, where A_f and A_d denote the bifurcation parameters. The clock regulates the sampling speed of chaotically encrypted duration, and then the chaotic duration sequence controls the sampling speed of chaotically encrypted frequency. Finally, a two-dimensional chaotic FDE sequence is generated. The Logistic map is adopted to generate a discrete time chaotic series [22], [23]. Accordingly, both the encrypted angular frequency ω_m and its encrypted duration D_m can be respectively expressed as:

$$\begin{cases} \omega_m = \gamma_i \omega_0 \\ D_{m\_q} = \beta_i D_0, \; q \in Z^+ \end{cases} \tag{8}$$

where γ_i and β_i are the chaotic security keys.

Generally, ω_0 and D_0 can be arbitrarily chosen based on the power level and transmission distance. Instead of simultaneously regulating both the transmitter's and the authorized receivers' matched capacitances by using switched-capacitor arrays [14], only the authorized receivers' ones need to be regulated as:

$$C_{sm}\left(\sum_{q=1}^{q=i} D_{m\_q}\right) = \frac{1}{\gamma_i^2} \cdot \frac{1}{\omega_0^2 L_{sm}} \tag{9}$$

which becomes a variable related with time and the encrypted frequency. Consequently, the encrypted energy package can only be decrypted by simultaneous regulation of the authorized receivers with knowledge of security keys.

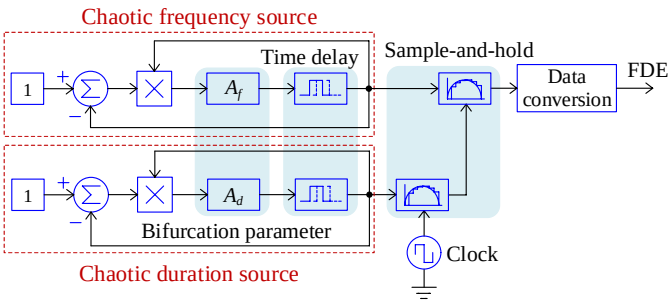

Fig. 2. Proposed two-dimensional chaotic FDE algorithm.

IV. Results and Verification

To illustrate the feasibility of the proposed FDE-WPT system using the switched-capacitorless transmitter, finite element analysis (FEA) and system simulation are performed. The design specifications and parameters are listed in Table I. In addition, an exemplified prototype is built for experimentation.

A. Simulation Results

Detailed geometries with dimensions of the transmitter and receiver coils are depicted in Fig. 3, where the transmission distance is 105 mm and each receiver coil can be separately controlled to pick up wireless power. By using FEA, the magnetic field distributions are shown in Fig. 4 in which only the central receiver coil is authorized (case 1) or only the right lateral receiver coil is authorized (case 2). It can be observed in Figs. 4(a) and (b) that the encryption scheme effectively builds up the magnetic flux pipe, and thus the vast majority of magnetic flux lines are bounded up through the authorized receiver coil and only extremely few ones are dispersed. Furthermore, Figs. 4(c) and (d) show the contour plots of the magnetic flux densities along the vertical plane, and the magnetic flux densities around the unauthorized receivers are extremely low. Figs. 4(e) and (f) depict the magnetic flux densities along the middle parallel plane, and the saddle-shape magnetic flux densities under the authorized receiver coil can respectively reach up to 0.255 mT and 0.251 mT.

Additionally, Fig. 5(a) demonstrates that the proposed scheme can achieve higher transmission efficiency as compared with the conventional one, which is due to the reduction of power loss. Meanwhile, the voltage stress across the transmitter's power switches of the proposed scheme (which is almost the same as the source voltage) is much lower than that of the conventional scheme (which reaches up to 2.36 times). On the other hand, Fig. 5(b) shows that the authorized receiver can successfully pick up the wireless power with the output voltage of 18 V, while the unauthorized receivers can only pick and generate insignificant values. Furthermore, the operating frequency and its active duration are simultaneously encrypted in a two-dimensional scale to enhance the energy security performance.

TABLE I
Design Specifications and Parameters

Items	Value
Transmitter coil turns (n_p)	24 N
Transmitter capacitance (C_p)	1.94 nF
Transmitter coil inductance (L_p)	1079 μH
Transmitter coil internal resistance(R_p)	0.8 Ω
Receiver coil turns (n_{sk})	27 N
Receiver capacitances (C_{s1}, C_{sm}, C_{sn})	9.92, 3.50~9.80, 9.68 nF
Receiver coil inductances (L_{s1}, L_{sm}, L_{sn})	352.33, 356.50, 350.04 μH
Receiver coil internal resistance (R_{sk})	0.35 Ω
Receiver operating frequency (f_k)	85.15~142.48 kHz
Load resistance (R_{Lk})	7.9 Ω
Output filter capacitance (C_o)	470 μF
Mutual inductances (L_{ps1}, L_{psm}, L_{psn})	71.70, 73.55, 75.70 μH

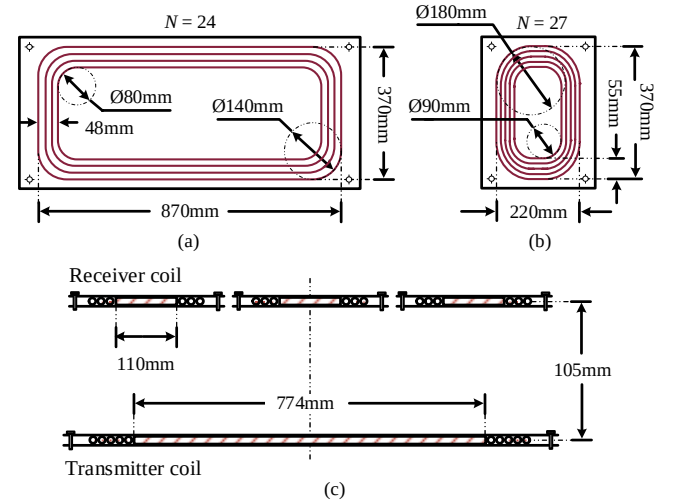

Fig. 3. Geometries of transmitter and receiver coils. (a) Transmitter coil. (b) Receiver coil. (c) Displacement among coils.

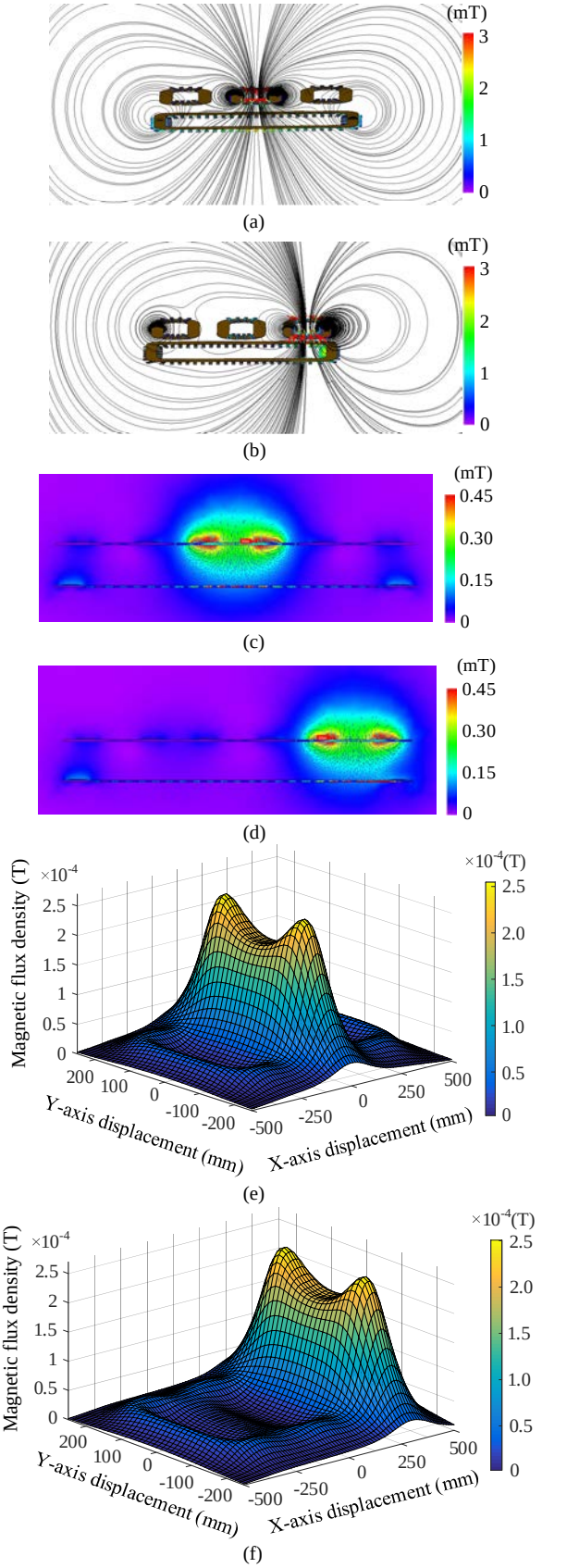

Fig. 4. Magnetic field distributions when central coil authorized (case 1) or lateral coil authorized (case 2). (a) Flux lines (case 1). (b) Flux lines (case 2). (c) Flux densities along vertical plane (case 1). (d) Flux densities along vertical plane(case 2). (e) Flux densities along middle parallel plane (case 1). (f) Flux densities along middle parallel plane (case 2).

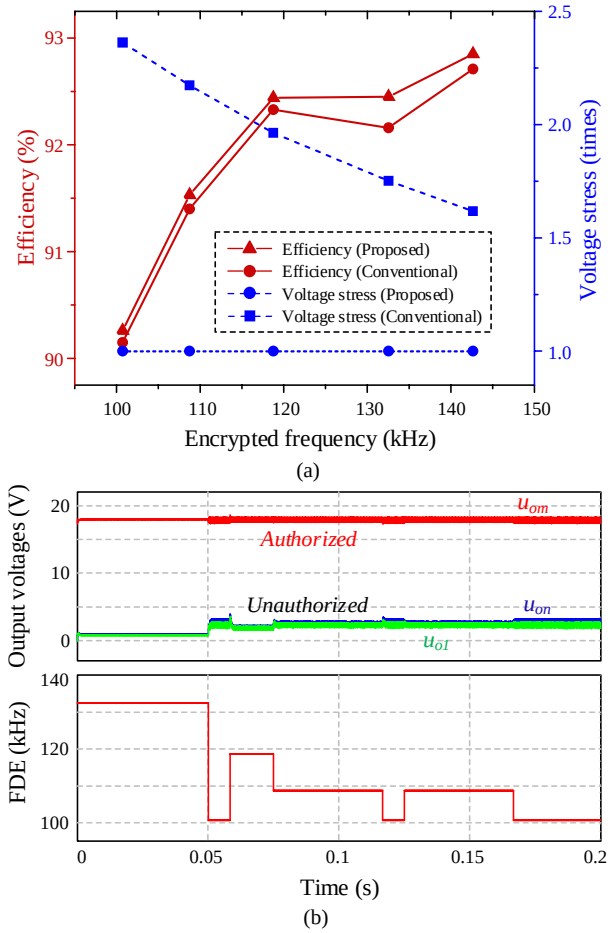

Fig. 5. Simulation performance of proposed FDE-WPT system. (a) Comparison of efficiencies and voltage stresses. (b) Security performance.

B. *Experimental Results*

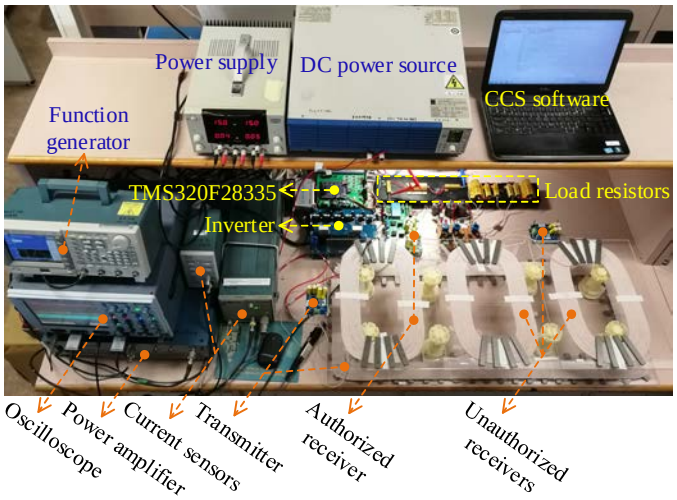

Fig. 6. Experimental setup.

To verify the feasibility of the proposed FDE-WPT system, an experimental setup is built as shown in Fig. 6. Then, Fig. 7 shows the measured waveforms of the transmitter current i_p and the receiver current i_{sm} at different operating frequencies with the same 220-V AC power source (which is realized by using a S-series RF power amplifier). It can be observed that there are high current ratios between i_p and i_{sm}, hence confirming the

merits of low power loss and high coil-to-coil transmission efficiency even when the transmitter operates at the non-resonant state.

In addition, Fig. 8(a) shows the encryption performance of the proposed FDE-WPT system at 185-V DC power source. It can be found that the output voltage u_{om} and current i_{sm} of the authorized receiver can achieve 18.7 V and 2.4 A, respectively, whereas the output voltages u_{o1} and u_{on} of the unauthorized ones are insignificant. The authorized receiver can pick up about 44.2 W with relatively high coil-to-coil transmission efficiency. Furthermore, the unauthorized receiver's performance is greatly suppressed, which indicates that the proposed two-dimensional FDE scheme is effective by flexibly encrypting the operating frequency and its duration in two-dimensional scale.

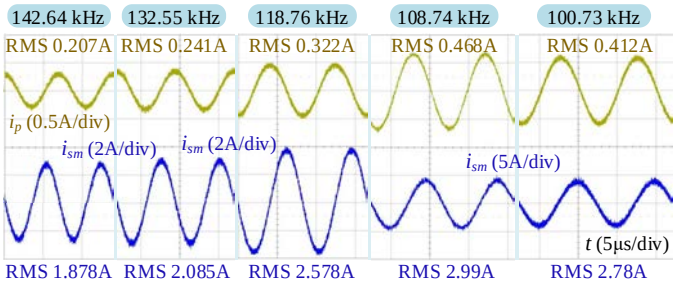

Fig. 7. Measured current waveforms of transmitter and authorized receivers at different operating frequencies.

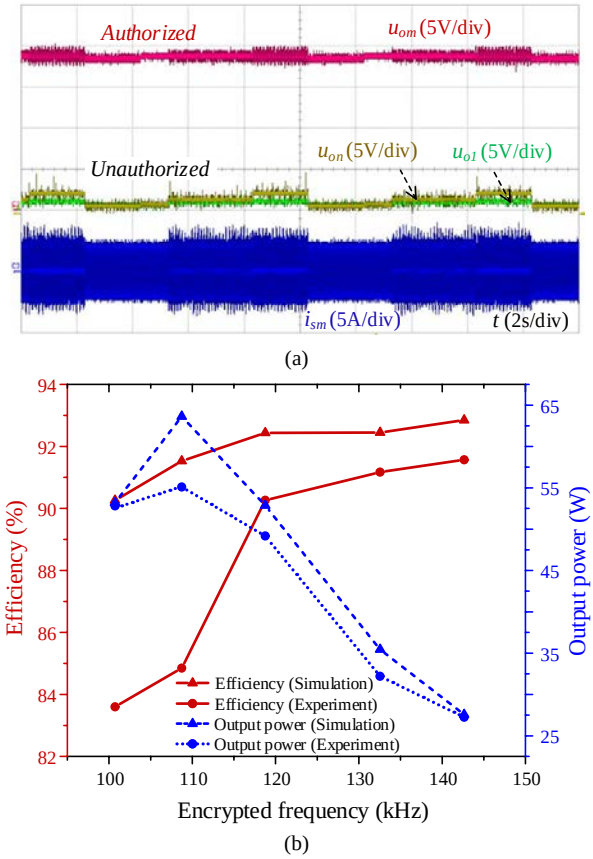

Fig. 8. Experimental performances of proposed system. (a) Output voltages and induced current. (b) Transmission efficiency and output power.

The measured transmission efficiency and output power of the proposed system at 220-V AC power source are plotted against the simulated results shown in Fig. 8(b). As expected, the measured transmission efficiency and output power are slightly lower than the simulated ones, which are actually due to inevitable power losses and drops across lines and contacts. Nevertheless, both the measured and simulated results have the same trends with respect to the encrypted frequency. Furthermore, it confirms that the MEBT and FDE can dynamically generate a sequence of security key to guarantee energy encryption while offering high-efficiency operation, namely always higher than 90.26% in simulation and 83.6% in experimentation. Thus, the proposed FDE-WPT system is well verified to improve the energy security performance for WPT while maintaining relatively high efficiency.

V. Conclusion

A switched-capacitorless energy-encrypted transmitter has been proposed and then implemented for roadway-charging EVs. The proposed two-dimensional chaotic FDE scheme generates a well-defended security key to improve the security performance. Moreover, by enhancing the mutual inductance and introducing the hybrid modulation, the proposed FDE-WPT system can offer high energy security while retaining high transmission efficiency which is always higher than 90.26% in simulation and 83.6% in experimentation. The feasibility of the proposed FDE-WPT system has been effectively verified by theoretical analysis, simulation and experimentation.

Acknowledgment

This work was supported by a grant (Project No. 17204317) from the Hong Kong Research Grants Council, Hong Kong Special Administrative Region, China.

References

[1] K. T. Chau, *Energy Systems for Electric and Hybrid Vehicles*. The IET, 2016.
[2] Z. Zhang, and K. T. Chau, "Homogeneous wireless power transfer for move-and-charge," *IEEE Trans. Power Electron.*, vol. 30, no. 11, pp. 6213-6220, Nov. 2015.
[3] Q. Zhu, L. Wang, Y. Guo, C. Liao, and F. Li, "Applying LCC compensation network to dynamic wireless EV charging system," *IEEE Trans. Ind. Electron.*, vol. 63, no. 10, pp. 6557-6567, Oct. 2016.
[4] A. A. S. Mohamed, A. A. Marim and O. A. Mohammed, "Magnetic design considerations of bidirectional inductive wireless power transfer system for EV applications," *IEEE Trans. Magn.*, vol. 53, no. 6, pp. 1-5, Jun. 2017.
[5] C. Jiang, K. T. Chau, T. W. Ching, C. Liu, and W. Han, "Time-division multiplexing wireless power transfer for separately excited DC motor drives," *IEEE Trans. Magn.*, vol. 53, no. 11, pp. 8205405:1-5 Nov. 2017.
[6] M. Sato, G. Yamamoto, D. Gunji, T. Imura and H. Fujimoto, "Development of wireless in-wheel motor using magnetic resonance coupling," *IEEE Trans. Power Electron.*, vol. 31, no. 7, pp. 5270-5278, Jul. 2016.
[7] W. Han, K. T. Chau, and Z. Zhang, "Flexible induction heating using magnetic resonant coupling," *IEEE Trans. Ind. Electron.*, vol. 64, no. 3, pp. 1982-1992, Mar. 2017.
[8] C. Jiang, K. T. Chau, Y. Leung, C. Liu, C. H. T. Lee, and W. Han, "Design and analysis of wireless ballastless fluorescent lighting," *IEEE Trans. Ind. Electron.*, DOI: 10.1109/TIE.2017.2784345.
[9] C. Liu, K. T. Chau, D. Wu, and S. Gao, "Opportunities and challenges of vehicle-to-home, vehicle-to-vehicle, vehicle-to-grid technologies," *Proc. IEEE*, vol. 101, no. 11, pp. 2409-2427, Nov. 2013.
[10] J. Shin, S. Shin, Y. Kim, S. Ahn, S. Lee, G. Jung, S.-J. Jeon, and D.-H. Cho, "Design and implementation of shaped magnetic-resonance-based wireless power transfer system for roadway-powered moving electric

vehicles," *IEEE Trans. Ind. Electron.*, vol. 61, no. 3, pp. 1179-1192, Mar. 2014.

[11] C. C. Mi, G. Buja, S. Y. Choi and C. T. Rim, "Modern advances in wireless power transfer Systems for roadway powered electric vehicles," *IEEE Trans. Ind. Electron.*, vol. 63, no. 10, pp. 6533-6545, Oct. 2016.

[12] Y. J. Kim, D. Ha, W. J. Chappell and P. P. Irazoqui, "Selective wireless power transfer for smart power distribution in a miniature-sized multiple-receiver system," *IEEE Trans. Ind. Electron.*, vol. 63, no. 3, pp. 1853-1862, Mar. 2016.

[13] Z. Zhang, K.T. Chau, C. Liu, C. Qiu and F. Lin, "An efficient wireless power transfer system with security considerations for electric vehicle applications," *J. Appl. Phys.*, vol. 115, no. 17, paper no. 17A328, pp. 1-3, May 2014.

[14] Z. Zhang, K. T. Chau, C. Qiu, and C. Liu, "Energy encryption for wireless power transfer," *IEEE Trans. Power Electron.*, vol. 30, no. 9, pp. 5237-5246, Sep. 2015.

[15] J. Tian, and A. P. Hu, "A DC-voltage-controlled variable capacitor for stabilizing the ZVS frequency of a resonant converter for wireless power transfer," *IEEE Trans. Power Electron.*, vol. 32, no. 3, pp. 2312-2318, Mar. 2017.

[16] Q. C. Zhong and Y. Zeng, "Control of inverters via a virtual capacitor to achieve capacitive output impedance," *IEEE Trans. Power Electron.*, vol. 29, no. 10, pp. 5568-5578, Oct. 2014.

[17] X. Chen, Y. Hou, S. C. Tan, C. K. Lee, and S. Y. R. Hui, "Mitigating voltage and frequency fluctuation in microgrids using electric springs," *IEEE Trans. Smart Grid*, vol. 6, no. 2, pp. 508-515, Mar. 2015.

[18] Y. Zhang, T. Lu, Z. Zhao, F. He, K. Chen, and L. Yuan, "Selective wireless power transfer to multiple loads using receivers of different resonant frequencies," *IEEE Trans. Power Electron.*, vol. 30, no. 11, pp. 6001-6005, Nov. 2015.

[19] L. Tan, J. Li, C. Chen, C. Yan, J. Guo, and X. Huang, "Analysis and performance improvement of WPT systems in the environment of single non-ferromagnetic metal plates," *Energies*, vol. 9, no. 8, p. 576, Jul. 2016.

[20] W. Liu, J. Zhang, and R. Chen, "Modelling and control of a novel zero-current-switching inverter with sinusoidal current output," *IET Power Electron.*, vol. 9, no. 11, pp. 2205-2215, Sep. 2016.

[21] X. Pan, A. Ghoshal, Y. Liu, Q. Xu, and A. K. Rathore, "Hybrid modulation based bidirectional electrolytic capacitor-less three-phase inverter for fuel cell vehicles: analysis, design, and experimental results," *IEEE Trans. Power Electron.*, DOI: 10.1109/TPEL.2017.2718731.

[22] Z. Zhang, K. T. Chau, Z. Wang, and W. Li, "Improvement of electromagnetic compatibility of motor drives using hybrid chaotic pulse width modulation," *IEEE Trans. Magn.*, vol. 47, no. 10, pp. 4018-4021, Oct. 2011.

[23] K. T. Chau, and Z. Wang, *Chaos in Electric Drive Systems – Analysis, Control and Application*. Wiley-IEEE Press, 2011.